

Edgar L Andreas\*

U.S. Army Cold Regions Research and Engineering Laboratory, Hanover, New Hampshire

and

Sinny Wang

Dartmouth College, Hanover, New Hampshire

## 1. INTRODUCTION

The significant wave height,  $H_{1/3}$ , is the average of the highest one-third of all waves occurring during a period. It is the most frequently reported wave statistic and, thus, appears often in ocean engineering and studies of sea surface physics. For example, the expected  $H_{1/3}$  environment is a design consideration for ships and ocean structures (Tucker and Pitt 2001, p. 164f.).  $H_{1/3}$  also arises in several applications that fall under the theme of this conference.  $H_{1/3}$  is a scaling depth that predicts the region over which bubbles are ejected and ocean turbulence is generated when waves break (e.g., Thorpe 1995).  $H_{1/3}$  can be used to predict the wave steepness and, in turn, the air-sea drag coefficient (Taylor and Yelland 2001; Fairall et al. 2003). And finally, our own specific interest in the significant wave height is that Andreas's (1992, 2003, 2004; Andreas and DeCosmo 2002) algorithm to predict the effects of sea spray on the air-sea heat fluxes requires  $H_{1/3}$ .

The Andreas (2003, 2004) algorithm uses the typical equilibrium-sea approximation (Kinsman 1965, p. 390f.; Earle 1979; Tucker and Pitt 2001, p. 100),

$$H_{1/3} = 0.030U_{10}^2, \quad (1)$$

to predict the significant wave height (in meters), where  $U_{10}$  is the wind speed (in  $\text{m s}^{-1}$ ) at a reference height of 10 m. But our recent meso-scale simulations of Atlantic storms (Perrie et al. 2005), which incorporated the Andreas (2003)

spray algorithm, hinted that (1) predicts waves that are too high. If this were true, the Andreas algorithm would predict latent heat fluxes mediated by spray that are too large.

We therefore looked at 18 years of hourly wave data from 12 different NOAA buoys off the northeast coast of the United States to investigate this issue. Figure 1 shows one year of such data and what (1) predicts. All 18 data sets resemble Fig. 1: In all cases, (1) overpredicts the average buoy measurements of  $H_{1/3}$  at high winds and predicts wave heights approaching zero as the wind speed approaches zero, while the data show

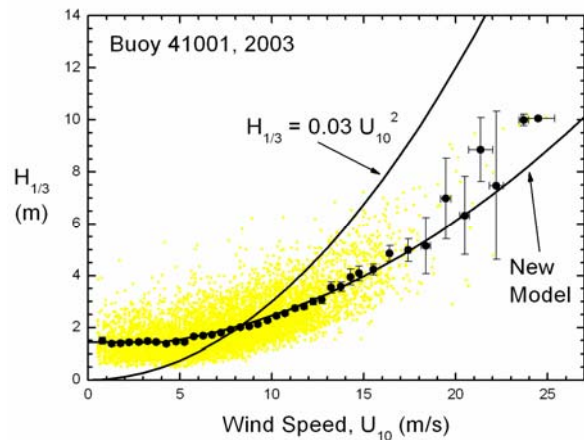


Figure 1. A year (2003) of hourly significant wave heights (yellow markers) from NOAA buoy 41001, which was 150 nm east of Cape Hatteras in water 4427 m deep. Black circles are wave heights averaged in wind speed bins that are  $0.5\text{m s}^{-1}$  wide; error bars are  $\pm 2$  standard deviations in the bin means. The curve marked “New Model” is our fit to these averages, equation (6). The curve labeled  $0.03U_{10}^2$  is a typical prediction for significant wave height in a fully developed sea.

\*Corresponding author address: Edgar L Andreas, U.S. Army Cold Regions Research and Engineering Laboratory, 72 Lyme Road, Hanover, New Hampshire 03755-1290; e-mail: [eandreas@crrel.usace.army.mil](mailto:eandreas@crrel.usace.army.mil).



Figure 2. A typical moored NOAA buoy that provided the data for this study.

that waves are always present, even in light winds. In the remainder of this paper, we fill in the details of this analysis and report our new parameterization for  $H_{1/3}$ .

## 2. MEASUREMENTS

The NOAA National Data Buoy Center (NDBC) operates scores of buoys in the oceans surrounding the United States. These buoys measure a host of meteorological and oceanographic variables; their hourly data, among other statistics, are archived at the NOAA NDBC website, [www.ndbc.noaa.gov](http://www.ndbc.noaa.gov). Figure 2 shows a typical NOAA NDBC ocean buoy. Gilhousen (1987) describes the design of these buoys and discusses some early testing of their measurements.

From this website, we obtained 18 years of data from 12 different buoys off the northeast coast of the United States. Figure 3 shows the locations of these buoys; Table 1 lists the specific aspects of the data sets we used in this study. From these data sets, we took only two variables, the wind speed and the significant wave height,  $H_{1/3}$ .

The buoys that provided the data for this study are pitch, roll, and heave buoys that use accelerometers and inclinometers to infer the wave spectrum through techniques such as those described in Tucker and Pitt (2001, p. 71ff.; cf. Gilhousen 1987). All wave calculations, including finding  $H_{1/3}$ , are done by microprocessors on each buoy, and the relevant wave statistics only are transmitted to shore.

Each of the buoys that we used measures wind speed with a propeller-vane at a height of 5 m (see Fig. 2). To standardize our analysis, we converted this reported wind speed,  $U_5$ , to the standard 10-m value,  $U_{10}$ , by assuming that all observations were in near-neutral stratification. In such conditions, the wind speed at height  $z$  obeys

$$U(z) = \frac{u_*}{k} \ln(z/z_0), \quad (2)$$

where  $u_*$  is the friction velocity,  $k$  ( $= 0.40$ ) is the von Kármán constant, and  $z_0$  is the roughness length. The wind speeds at 5 and 10 m are, thus, related by

$$U_{10} - U_5 = \frac{C_{DN10}^{1/2} U_{10}}{k} \ln(10/5), \quad (3)$$

or

$$U_{10} = \frac{U_5}{1 + \frac{C_{DN10}^{1/2}}{k} \ln(5/10)}, \quad (4)$$

where we use the usual definition of the neutral-stability drag coefficient at a reference height of 10 m,  $C_{DN10} = (u_* / U_{10})^2$ .

To complete (4), we use Large and Pond's (1982) result;

$$10^3 C_{DN10} = 1.14 \quad \text{for } U_{10} \leq 10 \text{ms}^{-1}, \quad (5a)$$

$$= 0.49 + 0.065 U_{10} \quad \text{for } 10 \text{ms}^{-1} \leq U_{10}. \quad (5b)$$

Although (5) requires  $U_{10}$ , we use  $U_5$  to compute  $C_{DN10}$  because this is the only wind speed we have available. For neutral stratification,  $U_5$  is typically about 6% less than  $U_{10}$ . Consequently, using  $U_5$  instead of  $U_{10}$  in (5) causes no inaccuracy for  $U_{10} \leq 10 \text{ms}^{-1}$  and biases our computed  $U_{10}$  values

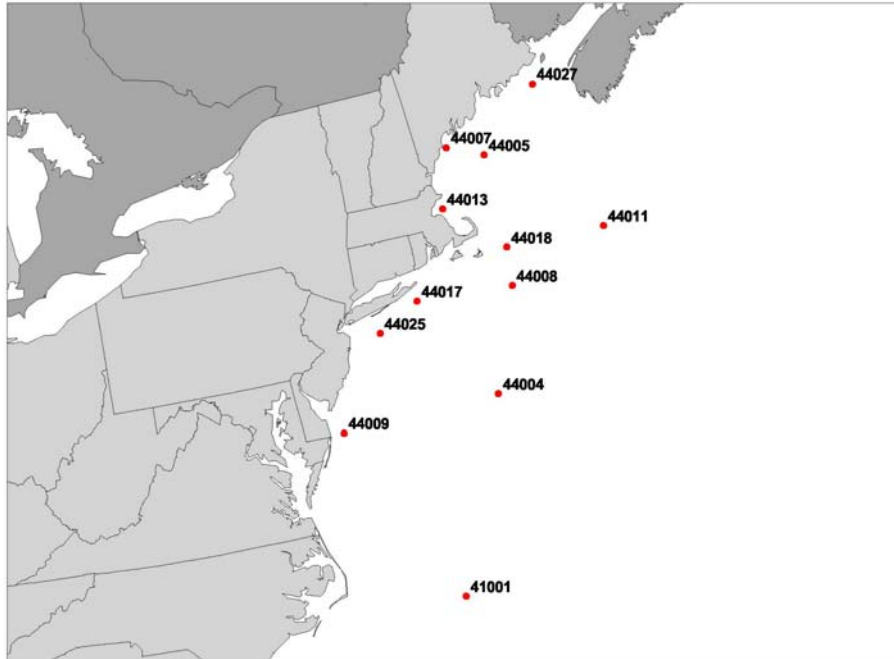


Figure 3. All data that we used in this study came from NOAA National Data Buoy Center buoys off the Atlantic coast of the United States.

low by less than 1% for wind speed above  $10\text{ms}^{-1}$ . Hence, our need to approximate  $U_{10}$  in (5) is not a problem.

Lastly, we screened the data files to eliminate missing or questionable data. If the reported wave height was  $H_{1/3} \leq 0.1\text{m}$ , we excluded the hour from our analysis. This test basically eliminated missing data. If  $U_5 < 0.5\text{ms}^{-1}$ , we also excluded the hour. This test eliminated hours with missing values for wind speed but also recognizes that propeller anemometers have some finite threshold starting speed. Propeller anemometers simply do not perform reliably in very light winds. Our visual screening of the data suggested that reported wind speeds below  $0.5\text{ms}^{-1}$  were suspect.

### 3. RESULTS

Figure 4 shows another plot like Fig. 1 to emphasize the similarities in wave behavior despite  $2\frac{1}{2}$  orders of magnitude difference in water depth between the two sites. In fact, all 18 years of data that we looked at yielded plots like those in Figs. 1 and 4. The average wave heights tend to be constant for 10-m winds less than

$4-5\text{ms}^{-1}$ ; and for winds nominally above  $10\text{ms}^{-1}$ , the observed wave heights are much less than the typical prediction for a local wind sea, (1).

We have, therefore, fitted all 18 data sets with a parameterization that has the form

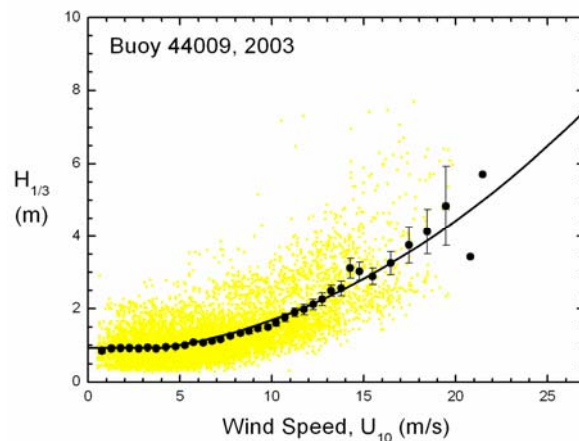


Figure 4. Similar to Fig. 1, except this is 2003 data from buoy 44009, which was in only 28 m of water 26 nm southeast of Cape May, NJ.

Table 1. Buoys used in this study and data years. “Number of Observations” shows how many screened hours of data were in each buoy record that we used in our analysis.  $\rho$  is the linear correlation coefficient between measured and modeled values of  $H_{1/3}$  for each year of data.

Buoy	Year	Latitude (°)	Longitude (°)	Water Depth (m)	Number of Observations	$\rho$
41001	2002	34.68	72.66	4426.8	8349	0.743
41001	2003	34.68	72.66	4426.8	7454	0.749
44004	2002	38.47	70.56	3124.4	8524	0.774
44004	2003	38.47	70.56	3124.4	8007	0.771
44005	2003	43.18	69.18	21.9	6930	0.778
44007	2002	43.53	70.14	18.9	8598	0.590
44007	2003	43.53	70.14	18.9	8246	0.567
44008	2002	40.50	69.43	62.5	8688	0.760
44008	2003	40.50	69.43	62.5	7478	0.736
44009	2003	38.46	74.70	28.0	8113	0.702
44011	2003	41.11	66.62	88.4	4587	0.738
44013	2002	42.35	70.69	55.0	8671	0.652
44013	2003	42.35	70.69	55.0	8492	0.646
44017	2003	40.70	72.00	44.8	8420	0.754
44018	2003	41.26	69.29	74.4	8534	0.718
44025	2002	40.25	73.17	36.3	8660	0.754
44025	2003	40.25	73.17	36.3	6629	0.755
44027	2003	44.27	67.31	182.0	5293	0.809

$$H_{1/3} = C(D) \quad \text{for } U_{10} \leq 4 \text{ ms}^{-1}, \quad (6a)$$

$$H_{1/3} = a(D)U_{10}^2 + b(D) \quad \text{for } 4 \text{ ms}^{-1} \leq U_{10}. \quad (6b)$$

heights for  $U_{10} \leq 4 \text{ ms}^{-1}$  by averaging all the wave heights in this wind speed range. Figure 5 shows the resulting  $C(D)$  value for each buoy record in our data set. The line we fitted to these values is

Here,  $H_{1/3}$  is in meters when  $U_{10}$  is in  $\text{m s}^{-1}$ , and  $D$  is the water depth.

To do this fitting, we first determined a depth-dependent constant value  $C(D)$  for the wave

$$C(D) = 1.36 \tanh \left[ \frac{\ln(D/6)}{1.9} \right], \quad (7)$$

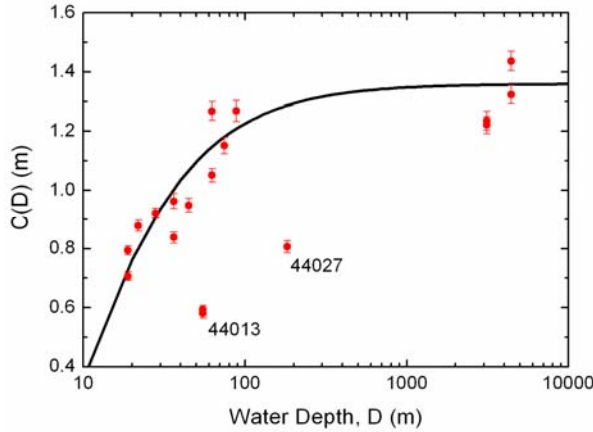


Figure 5. The height of the constant  $H_{1/3}$  region in each buoy record, obtained by averaging all wave heights for which  $U_{10} \leq 4 \text{ms}^{-1}$ . That is, the plot shows  $C$  in (6a) as function of water depth  $D$ . The error bars are  $\pm 2$  standard deviations in the mean of  $C$ . The line is (7), and we ignored buoys 44013 and 44027 as outliers in obtaining this fit.

which gives  $C$  in meters when  $D$  is in meters. In obtaining (7), we ignored three points in Fig. 5: the two years of data from buoy 44013 and the data from buoy 44027. Both buoys are in protected locations and see waves from only small sectors of open ocean. Buoy 44013 is outside Boston harbor; its only open ocean fetch is about an  $80^\circ$  sector to the northeast. Buoy 44027 is near the mouth of the Bay of Fundy and similarly sees only about a  $90^\circ$  sector to the open ocean.

We have good reason to suspect that  $H_{1/3}$  should go as the square of the wind speed in a wind sea—as (6b) suggests. Scaling arguments, as formulated, for example, by Kitaigorodskii (1973) and reiterated in Komen et al. (1994, p. 174f.) and Tucker and Pitt (2001, p. 100), suggest  $H_{1/3}$  should depend on  $U_{10}^2$  or  $u^2$ . We explore that suggestion with our data.

We found  $a(D)$  and  $b(D)$  in (6b) by two methods. Define  $\overline{H_{1/3}}$  as the average of all wave heights in a yearly buoy record for which  $U_{10} \geq 4 \text{ms}^{-1}$ . Define  $\overline{U_{10}^2}$  as the average of the squares of the corresponding wind speeds. Then

$$a'(D) = \frac{\overline{H_{1/3}} - C(D)}{\overline{U_{10}^2} - 16} \quad (8)$$

yields  $a(D)$  values in (6b) such that (6a) and (6b)

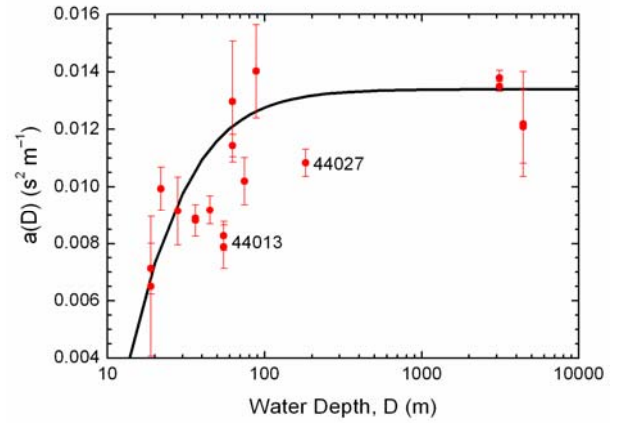


Figure 6. The wind speed multiplier  $a(D)$  in (6b) as a function of water depth,  $D$ . The error bars show  $\pm |a' - a''|$ , the absolute value of the difference in our two estimates of  $a(D)$ . The line is (11), although we ignored the points from buoys 44013 and 44027 as outliers in fitting this line.

are guaranteed to be continuous at  $U_{10} = 4 \text{ms}^{-1}$ . An estimate for  $b(D)$ , in meters, then comes from

$$b'(D) = C(D) - 16a'(D) . \quad (9)$$

Alternatively, we obtained  $a''(D)$  and  $b''(D)$  by simply doing a least-squares linear regression of  $H_{1/3}$  versus  $U_{10}^2$  for all  $U_{10} \geq 4 \text{ms}^{-1}$ . This fitting, however, does not necessarily require that (6a) and (6b) meet at  $U_{10} = 4 \text{ms}^{-1}$ , although our fitting generally produced results for (6b) that almost matched (6a).

To arrive at a consensus value for  $a(D)$  in (6b) for each buoy record, we simply averaged the  $a'(D)$  and  $a''(D)$  values. With this value, we then computed a  $b(D)$  value that guaranteed (6a) and (6b) to match at  $U_{10} = 4 \text{ms}^{-1}$  from

$$b(D) = C(D) - 16a(D) , \quad (10)$$

which again gives  $b$  in meters.

Figure 6 shows our best estimate of  $a(D)$  for each buoy, with error bars based on  $|a' - a''|$ . The line we have fitted by eye is

$$a(D) = 0.0134 \tanh \left[ \frac{\ln(D/9)}{1.3} \right] , \quad (11)$$

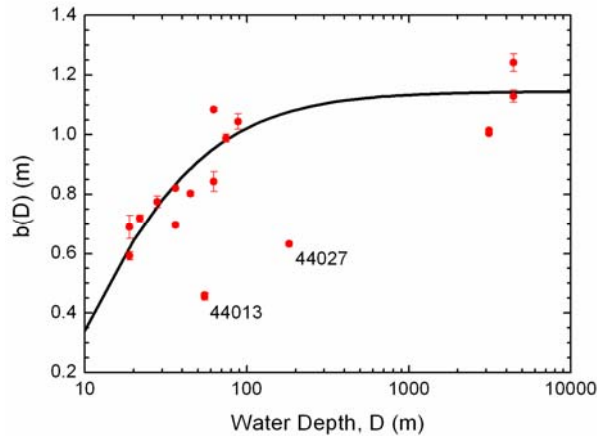


Figure 7. The additive constant  $b(D)$  in (6b) as a function of water depth,  $D$ . The error bars are  $\pm|b' - b''|$ , where  $b'$  and  $b''$  are the two estimates of  $b$  described in the text. The curve is (10) with (7) for  $C(D)$  and (11) for  $a(D)$ . Buoys 44013 and 44027 are again outliers.

which gives  $a(D)$  in  $\text{s}^2\text{m}^{-1}$  for water depth  $D$  in meters. As with Fig. 5, we ignored the results from buoys 44013 and 44027, which again appear as outliers because of their protected locations.

Finally, Fig. 7 shows our results for  $b(D)$ . Here, the fitting line is required by (10), with (7) and (11), respectively, as our functions for  $C(D)$  and  $a(D)$ . The error bars here are  $\pm|b' - b''|$ , where  $b'$  and  $b''$  are the two statistical estimates of  $b$  that we described above. Again, the results from buoys 44013 and 44027 are outliers on this plot, but we did not explicitly ignore these to obtain the curve in Fig. 7: It comes automatically for (10), (7), and (11).

To check the behavior of our parameterization, we used (7), (11), and (10) to compute  $C$ ,  $a$ , and  $b$ , respectively, for each buoy in our data set. We then used (6) to estimate  $H_{1/3}$  for each hour when we had observations of both wind speed and wave height. Figure 8, which is typical of these comparisons, shows measured and modeled values of  $H_{1/3}$  for one year of data (2002) from buoy 44008. The figure also shows the line for 1:1 correlation and the line obtained from least-squares regression for all the  $H_{1/3}$  pairs shown. Essentially, the best fit produced by (6) is almost indistinguishable from the 1:1 line. Figure 8 shows a distinct lower limit in modeled wave height because our algorithm will not predict  $H_{1/3}$  values less than  $C(D)$ .

The correlation coefficient for the measured-modeled  $H_{1/3}$  pairs in Fig. 8 is 0.760. Table 1 lists the correlation coefficients that we computed similarly for the other buoys in our data set. Most of the correlation coefficients are between 0.7 and 0.8; thus, our model typically explains 50–60% of the variance in the observed  $H_{1/3}$  values. Notice, the buoy with the shallowest water depth in our set, 44007 in 18.9 m of water, yielded the two lowest values for the correlation coefficient. Buoy 44007 was also the buoy nearest a shoreline. Buoy 44013, which we identified as an outlier in our set, yielded the next two lowest correlation coefficients. Ironically, though, buoy 44027, which is another outlier, produced the highest correlation coefficient; but the least-squared fit of the measured-modeled  $H_{1/3}$  pairs for this buoy deviated most from 1:1.

Several of the buoy records that we used include observations of  $H_{1/3}$  for 10-m wind speeds up to  $25 \text{ m s}^{-1}$ . Where we had such data, (6) still provided an accurate description of the correlation between  $H_{1/3}$  and  $U_{10}$ . Hence, we conclude that (6) is a reliable model of  $H_{1/3}$  for  $U_{10}$  up to, at least,  $25 \text{ m s}^{-1}$ .

#### 4. DISCUSSION AND CONCLUSIONS

Our analysis implies that the assumption of an equilibrium sea, which is the basis for obtaining wave statistics from the Pierson-Moskowitz spectrum, for instance (e.g., Tucker and Pitt 2001, p. 100), is rarely valid. This assumption yields models for the significant wave height that resemble (1). The multiplicative constant may be slightly different (cf. Tucker and Pitt 2001, p. 100; Taylor and Yelland 2001), but the analysis always predicts that  $H_{1/3}$  goes to zero as  $U_{10}$  goes to zero.

A very robust result of our analysis, in contrast, is that  $H_{1/3}$  is essentially independent of the local wind for  $U_{10} \leq 4 \text{ m s}^{-1}$  and is significantly larger, on average, than zero here. Figure 5 shows that this lower limit for  $H_{1/3}$  in light winds is a function of water depth. We presume that the waves constantly present, even in light winds, are from swell. An alternative explanation may be convectively induced wind gusts that can significantly enhance air-sea momentum transfer in light winds (e.g., Fairall et al. 1996). We are less enthusiastic about this explanation, though, because the mid-latitude locations for the buoys we studied may not produce large enough turbu-



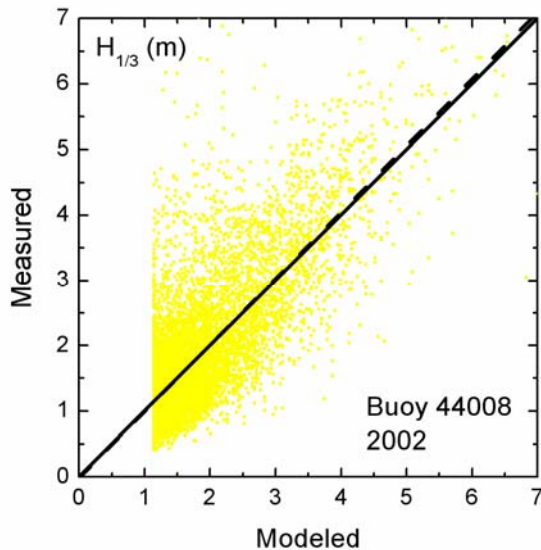


Figure 8. Measured and modeled values of  $H_{1/3}$  for buoy 44008 for all of 2002. This buoy is in 62.5 m of water 54 nm southeast of Nantucket. The solid line is the 1:1 relation; the dashed line is the least-squares fit. The correlation coefficient for the plotted values is 0.760.

lent surface heat fluxes to drive very gusty surface-level winds.

We cannot yet say how general our model—summarized in (6), (7), (10), and (11)—is. Since all of our buoys are off the U.S. east coast, all have a shoreline to their west; and with winds predominantly from the west here, the wave field at the buoys was often fetch-limited. Buoys off the U.S. west coast, in contrast, would usually see a wave field with unlimited fetch under, predominantly, westerly winds. Hence, we cannot yet rule out that the dependence we see on water depth may be an indirect effect of fetch.

Nevertheless, our analysis provides a framework for testing wind-wave parameterizations in other locations. It also strongly argues against using an equilibrium wind sea approximation—such as (1)—in models and analyses that require an estimate of  $H_{1/3}$  (e.g., Taylor and Yelland 2001; Fairall et al. 2003). This equilibrium approximation fails in two aspects: It underpredicts  $H_{1/3}$  in light winds and overpredicts it in winds, nominally, above  $10\text{ m s}^{-1}$ .

Finally, although our model requires only two parameters, wind speed and water depth, and is, thus, very simple compared to the sophistication common in other current wave models (e.g.,

Komen et al., 1994; Moon et al. 2004), it typically explains at least 50% of the variance in an observed record of significant wave height (Table 1). And in particular, it does very well in predicting long-term averages of  $H_{1/3}$  as a function of wind speed (Figs. 1 and 4).

## 5. ACKNOWLEDGMENTS

The U.S. Office of Naval Research supported this work with award N0001405MP20044. We thank Corinne M. Hirai for early help with the data processing and Stephen E. Belcher for helpful comments on our analysis.

## 6. REFERENCES

- Andreas, E. L., 1992: Sea spray and the turbulent air-sea heat fluxes. *J. Geophys. Res.*, **97**, 11,429–11,441.
- \_\_\_\_\_, 2003: An algorithm to predict the turbulent air-sea fluxes in high-wind, spray conditions. Preprints, *12th Conf. on Interactions of the Sea and Atmosphere*, Long Beach, CA, Amer. Meteor. Soc., CD-ROM 3.4, 7 pp.
- \_\_\_\_\_, 2004: A bulk air-sea flux algorithm for high-wind, spray conditions, Version 2.0. Preprints, *13th Conf. on Interactions of the Sea and Atmosphere*, Portland, ME, Amer. Meteor. Soc., CD-ROM P1.5, 8 pp.
- \_\_\_\_\_, and J. DeCosmo, 2002: The signature of sea spray in the HEXOS turbulent heat flux data. *Bound.-Layer Meteor.*, **103**, 303–333.
- Earle, M. D., 1979: Practical determinations of design wave conditions. *Ocean Wave Climate*, M. D. Earle and A. Malahoff, Eds., Plenum Press, 39–60.
- Fairall, C. W., E. F. Bradley, D. P. Rogers, J. B. Edson, and G. S. Young, 1996: Bulk parameterization of air-sea fluxes for Tropical Ocean-Global Atmosphere Coupled-Ocean Atmosphere Response Experiment. *J. Geophys. Res.*, **101**, 3747–3764.
- \_\_\_\_\_, \_\_\_\_\_, J. E. Hare, A. A. Grachev, and J. B. Edson, 2003: Bulk parameterization of air-sea fluxes: Updates and verification for the COARE algorithm. *J. Climate*, **16**, 571–591.
- Gilhousen, D. B., 1987: A field evaluation of NDBC moored buoy winds. *J. Atmos. Oceanic Technol.*, **4**, 94–104.
- Kinsman, B., 1965: *Wind Waves*. Prentice-Hall, 676 pp.

- Kitaigorodskii, S. A., 1973: *The Physics of Air-Sea Interaction*. A. Baruch, Trans., Israel Program for Scientific Translations, 237 pp.
- Komen, G. J., L. Cavaleri, M. Donelan, K. Hasselmann, S. Hasselmann, and P. A. E. M. Janssen, 1994: *Dynamics and Modelling of Ocean Waves*. Cambridge University Press, 532 pp.
- Large, W. G., and S. Pond, 1982: Sensible and latent heat flux measurements over the ocean. *J. Phys. Oceanogr.*, **12**, 464–482.
- Moon, I.-J., T. Hara, I. Ginis, S. E. Belcher, and H. L. Tolman, 2004: Effect of surface waves on air-sea momentum exchange. Part I: Effect of mature and growing seas. *J. Atmos. Sci.*, **61**, 2312–2333.
- Perrie, W., E. L. Andreas, W. Zhang, W. Li, J. Gyakum, and R. McTaggart-Cowan, 2005: Sea spray impacts on intensifying midlatitude cyclones. *J. Atmos. Sci.*, **62**, 1867–1883.
- Taylor, P. K., and M. J. Yelland, 2001: The dependence of sea surface roughness on the height and steepness of the waves. *J. Phys. Oceanogr.*, **31**, 572–590.
- Thorpe, S. A., 1995: Dynamical processes of transfer at the sea surface. *Prog. Oceanogr.*, **35**, 315–351.
- Tucker, M. J., and E. G. Pitt, 2001: *Waves in Ocean Engineering*. Elsevier, 521 pp.